

Gate-controlled localization to delocalization transition of flat band wavefunction in twisted monolayer—bilayer graphene

Siyu Li(李思宇), Zhengwen Wang(王政文), Yucheng Xue(薛禹承), Lu Cao(曹路), Kenji Watanabe, Takashi Taniguchi, Hongjun Gao(高鸿钧), and Jinhai Mao(毛金海)

Citation: Chin. Phys. B, 2023, 32 (**6**): 067304. DOI: 10.1088/1674-1056/acc805
Journal homepage: http://cpb.iphy.ac.cn; http://iopscience.iop.org/cpb

What follows is a list of articles you may be interested in

Machine learning of the *Γ*-point gap and flat bands of twisted bilayer graphene at arbitrary angles

Xiaoyi Ma(马宵怡), Yufeng Luo(罗宇峰), Mengke Li(李梦可), Wenyan Jiao(焦文艳), Hongmei Yuan(袁红梅), Huijun Liu(刘惠军), and Ying Fang(方颖)
Chin. Phys. B, 2023, 32 (**5**): 057306. DOI: 10.1088/1674-1056/acb2c3

Spin- and valley-polarized Goos-Hänchen-like shift in ferromagnetic mass graphene junction with circularly polarized light

Mei-Rong Liu(刘美荣), Zheng-Fang Liu(刘正方), Ruo-Long Zhang(张若龙), Xian-Bo Xiao(肖贤波), and Qing-Ping Wu(伍清萍)
Chin. Phys. B, 2023, 32 (**3**): 037301. DOI: 10.1088/1674-1056/ac89e2

Precisely controlling the twist angle of epitaxial MoS_2/graphene heterostructure by AFM tip manipulation

Jiahao Yuan(袁嘉浩), Mengzhou Liao(廖梦舟), Zhiheng Huang(黄智恒), Jinpeng Tian(田金朋), Yanbang Chu(褚衍邦), Luojun Du(杜罗军), Wei Yang(杨威), Dongxia Shi(时东霞), Rong Yang(杨蓉), and Guangyu Zhang(张广宇)
Chin. Phys. B, 2022, 31 (**8**): 087302. DOI: 10.1088/1674-1056/ac720e

Recent advances of defect-induced spin and valley polarized states in graphene

Yu Zhang(张钰), Liangguang Jia(贾亮广), Yaoyao Chen(陈瑶瑶), Lin He(何林), and Yeliang Wang(王业亮)
Chin. Phys. B, 2022, 31 (**8**): 087301. DOI: 10.1088/1674-1056/ac70c4

Half-metallicity induced by out-of-plane electric field on phosphorene nanoribbons

Xiao-Fang Ouyang(欧阳小芳) and Lu Wang(王路)
Chin. Phys. B, 2022, 31 (**7**): 077304. DOI: 10.1088/1674-1056/ac560d

---

RAPID COMMUNICATION

Gate-controlled localization to delocalization transition of flat band wavefunction in twisted monolayer–bilayer graphene

Siyu Li(李思宇)[1,2,†], Zhengwen Wang(王政文)[2,†], Yucheng Xue(薛禹承)[2], Lu Cao(曹路)[3], Kenji Watanabe[4], Takashi Taniguchi[4], Hongjun Gao(高鸿钧)[1,2], and Jinhai Mao(毛金海)[2,‡]

[1] *Institute of Physics, Chinese Academy of Sciences, Beijing* 100190, *China*

[2] *School of Physical Sciences and CAS Center for Excellence in Topological Quantum Computation, University of Chinese Academy of Sciences, Beijing* 100049, *China*

[3] *College of Materials Science and Optoelectronic Technology, Center of Materials Science and Optoelectronics Engineering, University of Chinese Academy of Sciences, Beijing* 100049, *China*

[4] *Advanced Materials Laboratory, National Institute for Materials Science, Tsukuba* 305-0044, *Japan*

(Received 7 February 2023; revised manuscript received 24 March 2023; accepted manuscript online 28 March 2023)

Twisted graphene systems with flat bands have attracted much attention for they are excellent platforms to research novel quantum phases. Recently, transport measurements about twisted monolayer–bilayer graphene (tMBG) have shown the existence of correlated states and topological states in this system. However, the direct observations of the band structures and the corresponding spatial distributions are still not sufficient. Here we show that the distributions of flat bands in tMBG host two different modes by scanning tunneling microscopy and spectroscopy (STM/S). By tuning our tMBG device from the empty filling state to the full filling state through the back gate, we observe that the distributions of two flat bands develop from localized mode to delocalized mode. This gate-controlled flat band wavefunction polarization is unique to the tMBG system. Our work suggests that tMBG is promising to simulate both twisted bilayer graphene (TBG) and twisted double bilayer graphene (tDBG) and would be an ideal platform to explore novel moiré physics.

Keywords: graphene, Van der Waals heterostructures, scanning tunneling microscopy/spectroscopy

PACS: 73.22.Pr, 68.37.Ef, 85.30.Tv **DOI:** 10.1088/1674-1056/acc805

1. Introduction

Van der Waals heterostructures with tiny twist angle between the atom-thin layers have emerged as ideal platforms for the research of novel quantum phases which are highly tunable by external fields.[1,2] In graphene-based moiré systems, renormalized band structures host energetically narrow bands, called flat bands, which boost the electron correlation strength to overwhelm the kinetic energy.[3] By tuning the doping level of flat bands, many correlated phenomena have been reported. In twisted bilayer graphene (TBG) with magic angle ($\sim 1.1^\circ$), which hosts spatially localized flat bands, correlated insulating states, unconventional superconductivity and Chern insulating states have been observed.[4–9] In twisted double bilayer graphene (tDBG), which hosts spatially delocalized flat bands, transport measurements have revealed the spin-polarized correlated states and superconductivity-like states.[10–13]. Also, twisted monolayer–bilayer graphene (tMBG), in which a monolayer graphene is twisted with an AB-stacking Bernal bilayer graphene, has been predicted to be a flat-band moiré system with a high degree of tunability to realize exotic quantum phases. With reduced spatial symmetry, tMBG has been proved to contain topological flat bands, and the electrically tunable correlated states and ferromagnetism have been observed in transport measurements.[14–17] Up to now, most investigations about tMBG are focused on the transport properties, but the microscopic mechanism of the system's electronic structures is obscure. To deeply understand the rich correlated and topological physics in tMBG, directly measurements about the band structures and their responds to the external fields and doping level are needed.

Here we use scanning tunneling microscopy and spectroscopy (STM and STS) to study the electronic properties of twisted monolayer–bilayer graphene (tMBG) devices, whose structures allow us to continuously tune the electron filling and the electric field in our tMBG samples. By probing the local density of states (LDOS) at full electron filling and empty electron filling, we observe two moiré bands with narrow bandwidth which are referred to as the valence flat band (VFB) and the conduction flat band (CFB). Also, we find that in real space these two flat bands show delocalization behavior at full electron filling and localization behavior at empty electron filling. This phenomenon consists with theoretical predictions that tMBG resembles either TBG (with spatially localized flat bands) or tDBG (with spatially delocalized flat bands) depending on the direction of displacement field $\boldsymbol{D}$.[16] Our results suggest that tMBG hosts highly tunable electronic structure to

[†] These authors contributed equally to this work.

[‡] Corresponding author. E-mail: jhmao@ucas.ac.cn

© 2023 Chinese Physical Society and IOP Publishing Ltd

simulate TBG and tDBG, and tMBG is an elegant platform for the study of novel physics found in graphene-based moiré systems.

2. Sample fabrication and methods

We fabricated our tMBG samples by a tear-and-stack technique and finally deposited the tMBG/hBN (hexagonal boron nitride) stack onto a SiO_2/Si wafer.[7,18] With hBN and SiO_2 as dielectric layers, we could apply a back gate voltage V_g to the devices, then change the carrier density n and the perpendicular displacement field $\boldsymbol{D}$ in the devices. The STM experiments were performed with an ultrahigh vacuum STM (Createc, $\sim 10^{-10}$ mbar) at 4.8 K. Before performing the measurements on tMBG, the system and STM tip were checked on $NbSe_2$, where the charge density wave (CDW) and superconducting gaps were used for calibrations. The STM images were acquired under constant current mode with the sample biased (50 pA, -1 V) and the $\mathrm{d}I/\mathrm{d}V$ spectra were gained by standard lock-in technique, with 3 mV AC modulation added on the DC sample bias.

3. Results and discussion

Figure 1(a) shows the sketch of our device for the STM measurements and Fig. 1(b) shows the microscope details of the tMBG stack. The moiré patterns of tMBG have three distinct stackings orders called ABB, ABA and ABC.[16] Figure 1(c) is the STM topographic image of the tMBG, three regions with different contrast can be seen clearly within the moiré unit cell corresponding to the ABB, ABA and ABC regions.[16] We can directly measure the moiré wavelength of ~ 14 nm (Fig. 1(d)), which corresponds to the twisted angle of $\theta \sim 1^\circ$ according to the formula $l = a/\theta$, where l is the moiré wavelength, $a = 0.246$ nm is the lattice constant of graphene and θ is the twisted angle.[19]

Next, we perform $\mathrm{d}I/\mathrm{d}V$ spectroscopy measurements in ABB, ABA and ABC regions when the flat bands are completely full or empty with electrons. Figure 2(a) shows the $\mathrm{d}I/\mathrm{d}V$ spectra in ABB, ABA and ABC regions at back-gate voltage $V_g = -30$ V, and at this situation the displacement field $\boldsymbol{D}$ points from bilayer to monolayer graphene. From these STS curves, we observe two energetically narrow peaks, both of which have a full width at half maximum (FWHM) of ~ 20 meV, within the bias range from 10 meV to 50 meV. We label the two peaks as the valence flat band (VFB) and the conduction flat band (CFB). At $V_g = -30$ V, these two flat bands are completely empty because they are above the Fermi level (dashed line in Fig. 2(a)). Comparing these curves, we find that the intensities of VFB and CFB in ABB region are larger than that in ABA and ABC regions, and the intensities in ABA region are almost the same in ABC region. This prominent feature suggests that the flat bands are mostly localized in ABB region and it is very similar with what has been observed in the twisted bilayer graphene (TBG)[7–9,20] by STM experiments. In order to delineate this feature more precisely, we calculate the area under flat bands of the $\mathrm{d}I/\mathrm{d}V$ spectra in the three regions, add them together and then calculate the area ratios R_{area} for the ABB, ABA and ABC regions, respectively. The value of R_{area} can quantitively show the localization of flat bands. For example, if $R_{\mathrm{ABB}} = 1$ and $R_{\mathrm{ABA}} = R_{\mathrm{ABC}} = 0$ (the value of $R_{\mathrm{ABB}} + R_{\mathrm{ABA}} + R_{\mathrm{ABC}}$ is always 1, which is normalized by the superlattice unit cell), it means that the VFB and the CFB are completely localized in ABB regions. The histogram of calculated area ratios R_{area} for the three regions in Fig. 2(b) clearly demonstrates that the two flat bands are mainly localized in ABB regions and reside evenly but slightly in ABA and ABC regions. The $\mathrm{d}I/\mathrm{d}V$ maps ($V_g = -30$ V) obtained at the VFB peak energy ($V_{\mathrm{bias}} = 19$ meV) and the CFB peak energy ($V_{\mathrm{bias}} = 39$ meV), shown in Fig. 2(c), further confirm that the two flat bands are localized in ABB region. We conclude that at empty electron filling the spatial distribution of flat bands in tMBG is highly localized and resembles the distribution of flat bands in TBG.

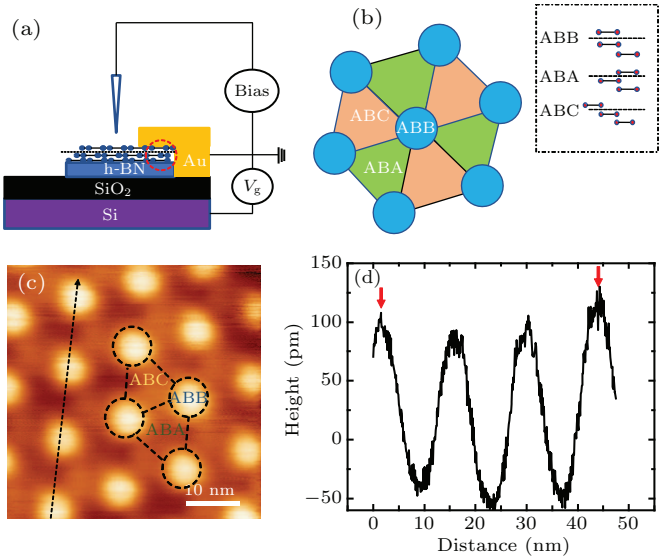


Fig. 1. (a) The sketch of the twisted monolayer–bilayer graphene (tMBG) device with a back gate to tune the device doping and external electric field. (b) The configuration of tMBG moiré pattern consisting with three stacking orders called ABB, ABA and ABC, and their atomic structures are showed in the dashed box. (c) The STM topographic image of tMBG ($V_{\mathrm{bias}} = -1$ V, $I_{\mathrm{setpoint}} = 50$ pA). The dashed lines and circles outline the moiré unit cell and the ABB, ABA and ABC regions. (d) The line-profile along dashed arrow in (c), showing the height of topography changes. From it a twisted angle $\theta \sim 1^\circ$ can be calculated.

Then we tune back-gate voltage V_g to 35 V. As seen in Fig. 3(a), the $\mathrm{d}I/\mathrm{d}V$ spectra in ABB and ABA regions still host two narrow peaks in the bias range from -80 meV to -20 meV, which correspond to the VFB and CFB. The spectrum in ABC region is a little more complex for its VFB splitting to two branches. The splitting of VFB in ABC region is related to the correlation effect and would not impede the following analysis.[21] At $V_g = 35$ V, the VFB and CFB are

fully filled with electrons for they are well below the Fermi level (dashed line in Fig. 3(a)). The change of the back gate voltage from −30 V to 35 V not only tunes the doping of the flat bands (from empty state to full state), but also reverses the direction of displacement filed $\boldsymbol{D}$ in the sample. Under a back gate voltage of 35 V, the displacement field $\boldsymbol{D}$ points from monolayer to bilayer graphene. The most striking characteristic of the $\mathrm{d}I/\mathrm{d}V$ spectra of the three regions now is that they host comparable peak intensities of the flat bands, which is distinct from the observation at $V_\mathrm{g} = -30$ V. To show this phenomenon quantitively, we calculate the area ratios R_area for ABB, ABA and ABC regions as above. The histogram of calculated area ratios R_area for the three regions in Fig. 3(b) shows similar results, which indicate the two flat bands extend in real space. Interestingly, the spatial delocalization of flat bands has already been reported in the STM experiments and transport measurements of tDBG.[22–24] Figure 3(c) shows the $\mathrm{d}I/\mathrm{d}V$ maps ($V_\mathrm{g} = 40$ V) obtained at the CFB peak energy ($V_\mathrm{bias} = -38$ meV) and the VFB peak energy ($V_\mathrm{bias} = -74$ meV), both of them demonstrate that VFB and CFB delocalize in the real space. Therefore, at the full filling state, the spatial distribution of the two flat bands in tMBG is delocalized and similar to the distribution of flat bands in tDBG.

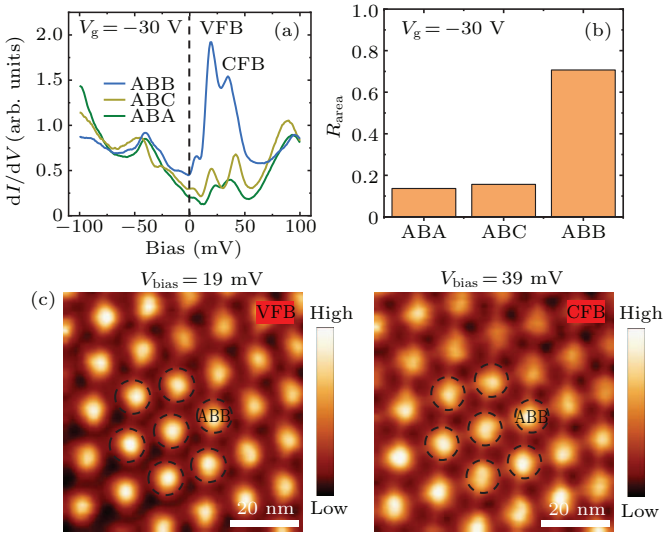


Fig. 2. (a) The $\mathrm{d}I/\mathrm{d}V$ spectra measured in ABA, ABC and ABB stackings under back-gate voltage $V_\mathrm{g} = -30$ V ($V_\mathrm{bias} = -100$ mV, $I_\mathrm{setpoint} = 200$ pA). (b) Histogram of the R_area at ABA, ABC and ABB directly calculated from (a). (c) $\mathrm{d}I/\mathrm{d}V$ maps (under back-gate voltage $V_\mathrm{g} = -30$ V) at $V_\mathrm{bias} = 19$ mV and 39 mV, which correspond to the VFB and CFB. The dashed circles outline ABB regions.

Phenomenologically, tMBG can be viewed as the transition state from TBG to tDBG. It seems naturally that tMBG system would host electronic structures similar both with TBG and tDBG. Correlated states have been reported in both TBG and tDBG, but the mechanism is different from each other for they host distinct spatial distributions of flat bands.[4,8,20] In TBG the localized flat bands in the AA stacking region have suggested the Mott-like origin of the correlation-driven phases.[4] But in tDBG the spatially delocalized flat bands indicate that the correlated states may stem from the non-local exchange interaction.[23] For the observed correlated states in tMBG, its mechanism is still under exploring.[18] Our experiments revealing the localization–delocalization transition of the spatial distributions of the flat bands in tMBG can give a hint on it.

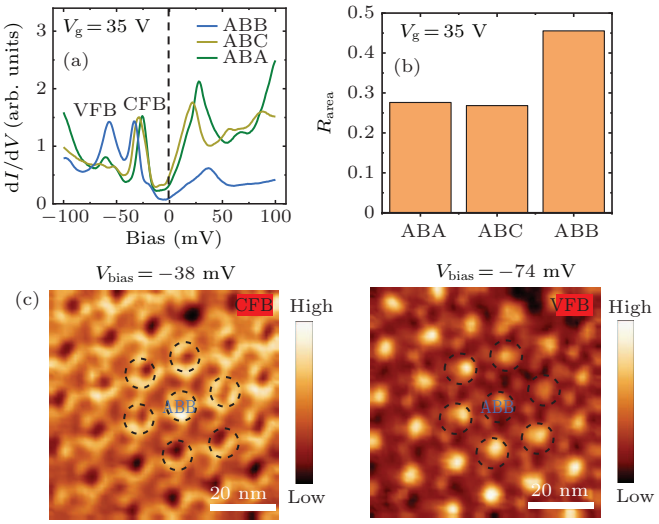


Fig. 3. (a) The $\mathrm{d}I/\mathrm{d}V$ spectra measured in ABA, ABC and ABB stackings under back-gate voltage $V_\mathrm{g} = 35$ V ($V_\mathrm{bias} = -100$ mV, $I_\mathrm{setpoint} = 200$ pA). (b) Histogram of the R_area at ABA, ABC and ABB directly calculated from (a). (c) $\mathrm{d}I/\mathrm{d}V$ maps (under back-gate voltage $V_\mathrm{g} = 40$ V) at $V_\mathrm{bias} = -74$ mV and −38 mV, which correspond to the VFB and CFB. The dashed circles outline ABB region.

4. Conclusion

In summary, we directly visualize the flat bands and their spatial distributions in tMBG via STM and STS. By using the back gate to dope the system from the empty filling state to the full filling state, amazing transition of the spatial distributions of flat bands from localization to delocalization happens. In the empty filling state tMBG behaviors like TBG and in the full filling state tMBG behaviors like tDBG. This phenomenon is unique to the tMBG system for both in TBG and tDBG no such transition has been reported. Our experiment unveils that with its highly tunable band structures tMBG would be an important platform to further study the moiré physics of twisted graphene systems.

Acknowledgments

We acknowledge support from the National Key R&D Program of China (Grant No. 2019YFA0307800), Beijing Natural Science Foundation (Grant No. Z190011), the National Natural Science Foundation of China (Grant No. 11974347), and Fundamental Research Funds for the Central Universities.

References

[1] Novoselov K S, Mishchenko A, Carvalho A and Castro Neto A H 2016 *Science* **353** aac9439
[2] Geim A K and Grigorieva I V 2013 *Nature* **499** 419
[3] Bistritzer R and MacDonald A H 2011 *Proc. Natl. Acad. Sci. USA* **108** 12233
[4] Cao Y, Fatemi V, Demir A, Fang S, Tomarken S L, Luo J Y, Sanchez-Yamagishi J D, Watanabe K, Taniguchi T, Kaxiras E, Ashoori R C and Jarillo-Herrero P 2018 *Nature* **556** 80
[5] Cao Y, Fatemi V, Fang S, Watanabe K, Taniguchi T, Kaxiras E and Jarillo-Herrero P 2018 *Nature* **556** 43
[6] Nuckolls K P, Oh M, Wong D, Lian B, Watanabe K, Taniguchi T, Bernevig B A and Yazdani A 2020 *Nature* **588** 610
[7] Jiang Y, Lai X, Watanabe K, Taniguchi T, Haule K, Mao J and Andrei E Y 2019 *Nature* **573** 91
[8] Kerelsky A, McGilly L J, Kennes D M, Xian L, Yankowitz M, Chen S, Watanabe K, Taniguchi T, Hone J, Dean C, Rubio A and Pasupathy A N 2019 *Nature* **572** 95
[9] Xie Y, Lian B, Jack B, Liu X, Chiu C L, Watanabe K, Taniguchi T, Bernevig B A and Yazdani A 2019 *Nature* **572** 101
[10] Burg G W, Zhu J, Taniguchi T, Watanabe K, MacDonald A H and Tutuc E 2019 *Phys. Rev. Lett.* **123** 197702
[11] Shen C, Chu Y, Wu Q, Li N, Wang S, Zhao Y, Tang J, Liu J, Tian J, Watanabe K, Taniguchi T, Yang R, Meng Z Y, Shi D, Yazyev O V and Zhang G 2020 *Nat. Phys.* **16** 520
[12] Liu X, Hao Z, Khalaf E, Lee J Y, Ronen Y, Yoo H, Haei Najafabadi D, Watanabe K, Taniguchi T, Vishwanath A and Kim P 2020 *Nature* **583** 221
[13] Cao Y, Rodan-Legrain D, Rubies-Bigorda O, Park J M, Watanabe K, Taniguchi T and Jarillo-Herrero P 2020 *Nature* **583** 215
[14] Xu S, Al Ezzi M M, Balakrishnan N, Garcia-Ruiz A, Tsim B, Mullan C, Barrier J, Xin N, Piot B A, Taniguchi T, Watanabe K, Carvalho A, Mishchenko A, Geim A K, Fal'ko V I, Adam S, Neto A H C, Novoselov K S and Shi Y 2021 *Nat. Phys.* **17** 619
[15] Rademaker L, Protopopov I V and Abanin D A 2020 *Phys. Rev. Res.* **2** 033150
[16] Chen S, He M, Zhang Y H, Hsieh V, Fei Z, Watanabe K, Taniguchi T, Cobden D H, Xu X, Dean C R and Yankowitz M 2020 *Nat. Phys.* **17** 374
[17] Polshyn H, Zhu J, Kumar M A, Zhang Y, Yang F, Tschirhart C L, Serlin M, Watanabe K, Taniguchi T, MacDonald A H and Young A F 2020 *Nature* **588** 66
[18] Li S Y, Wang Z, Xue Y, Wang Y, Zhang S, Liu J, Zhu Z, Watanabe K, Taniguchi T, Gao H J, Jiang Y and Mao J 2022 *Nat. Commun.* **13** 4225
[19] Lopes Dos Santos J M, Peres N M and Castro Neto A H 2007 *Phys. Rev. Lett.* **99** 256802
[20] Wong D, Nuckolls K P, Oh M, Lian B, Xie Y, Jeon S, Watanabe K, Taniguchi T, Bernevig B A and Yazdani A 2020 *Nature* **582** 198
[21] Choi Y, Kemmer J, Peng Y, Thomson A, Arora H, Polski R, Zhang Y, Ren H, Alicea J, Refael G, von Oppen F, Watanabe K, Taniguchi T and Nadj-Perge S 2019 *Nat. Phys.* **15** 1174
[22] Rubio-Verdú C, Turkel S, Song Y, Klebl L, Samajdar R, Scheurer M S, Venderbos J W F, Watanabe K, Taniguchi T, Ochoa H, Xian L, Kennes D M, Fernandes R M, Rubioá and Pasupathy A N 2021 *Nat. Phys.* **18** 196
[23] Zhang C, Zhu T, Kahn S, Li S, Yang B, Herbig C, Wu X, Li H, Watanabe K, Taniguchi T, Cabrini S, Zettl A, Zaletel M P, Wang F and Crommie M F 2021 *Nat. Commun.* **12** 2516
[24] Kashiwagi M, Taen T, Uchida K, Watanabe K, Taniguchi T and Osada T 2022 *Jpn. J. Appl. Phys.* **61** 100907